Available online at www.sciencedirect.com
SCIENCE DIRECT®
International Journal of Pharmaceutics 269 (2004) 509–522
international journal of pharmaceutics
www.elsevier.com/locate/ijpharm

Physicochemical properties and mechanism of drug release from ethyl cellulose matrix tablets prepared by direct compression and hot-melt extrusion

Michael M. Crowley [a,*], Britta Schroeder [b], Anke Fredersdorf [b], Sakae Obara [c], Mark Talarico [d], Shawn Kucera [a], James W. McGinity [a]

[a] *Division of Pharmaceutics, College of Pharmacy, The University of Texas at Austin, Austin, TX 78712, USA*
[b] *College of Pharmacy, Freie Universität Berlin, Berlin, Germany*
[c] *Shin-Etsu Chemical Co. Ltd., Specialty Chemicals Research Center, Niigata 942-8601, Japan*
[d] *Micromeritics Instrument Corp., One Micromeritics Drive, Norcross, GA 30093-1877, USA*

Received 19 March 2003; received in revised form 16 September 2003; accepted 26 September 2003

Abstract

The objective of this research project was to determine the physicochemical properties and investigate the drug release mechanism from ethyl cellulose (EC) matrix tablets prepared by either direct compression or hot-melt extrusion (HME) of binary mixtures of water soluble drug (guaifenesin) and the polymer. Ethyl cellulose was separated into "fine" or "coarse" particle size fractions corresponding to 325–80 and 80–30 mesh particles, respectively. Tablets containing 30% guaifenesin were prepared at 10, 30, or 50 kN compaction forces and extruded at processing temperatures of 80–90 and 90–110 °C. The drug dissolution and release kinetics were determined and the tablet pore characteristics, tortuosity, thermal properties and surface morphologies were studied using helium pycnometry, mercury porosimetry, differential scanning calorimetry and scanning electron microscopy. The tortuosity was measured directly by a novel technique that allows for the calculation of diffusion coefficients in three experiments. The Higuchi diffusion model, Percolation Theory and Polymer Free Volume Theory were applied to the dissolution data to explain the release properties of drug from the matrix systems. The release rate was shown to be dependent on the ethyl cellulose particle size, compaction force and extrusion temperature.

Keywords: Hot-melt extrusion; Guaifenesin; Ethyl cellulose; Matrix tablets; Higuchi diffusion model; Porosity; Tortuosity; Percolation; Free volume; Sustained release; Mercury porosimetry

1. Introduction

Ethyl cellulose (EC) is a non-toxic, stable, compressible, inert, hydrophobic polymer that has been widely used to prepare pharmaceutical dosage forms. The properties of ethyl cellulose sustained release products, including film coated tablets (Rowe, 1992), microspheres (Akbuga, 1991; Eldridge et al., 1990), microcapsules (Jalsenjak et al., 1977) and matrix tablets for both soluble and poorly soluble drugs (Shaikh et al., 1987a,b) have been reported.

Hot-melt extrusion (HME) is a widely used process in the plastics industry to produce tubing, pipes and films. In pharmaceutical systems, HME has been

* Corresponding author. Tel.: +1-512-471-6834; fax: +1-512-471-7474.
E-mail address: mmcrowley@mail.utexas.edu (M.M. Crowley).

0378-5173/$ – see front matter © 2003 Elsevier B.V. All rights reserved.
doi:10.1016/j.ijpharm.2003.09.037

used to prepare granules, sustained-release tablets, and transdermal drug delivery systems (AitkenNichol et al., 1996; Follonier et al., 1994; McGinity et al., 2000; Zhang and McGinity, 1999, 2000). It has been demonstrated that the processing method can dictate the porosity and pore structure of the dosage form (Selkirk and Ganderton, 1970; Zoglio and Carstensen, 1983). Previous workers have also shown that thermal processing results in a more tortuous product (Rubio and Ghaly, 1994; Zhang et al., 2001).

Several researchers have suggested that diffusion controlled sustained release dosage forms prepared by HME have slower drug release rates than those prepared by traditional methods due to lower porosity and higher tortuosity (Young et al., 2002). Polymeric materials are softened or molten during hot-melt extrusion and subjected to intense mixing resulting in the generation of high pressures. Air present in the powder bed can be excluded from the polymer melt during hot-melt extrusion. As a result, HME dosage forms are expected to have a lower porosity and higher tortuosity, in comparison with the dosage forms prepared by tabletting processes.

The Higuchi Square Root Model (Higuchi, 1963) has been successfully applied to model the kinetics of drug release from matrix systems. The Eq. (1) was derived from Fick's Law of diffusion and applied to porous hydrophobic polymeric drug delivery systems in homogenous matrices and granular matrices.

$$Q(t) = \sqrt{D_s C_a \frac{\varepsilon}{t}(2C_0 - \varepsilon C_a)t} = \sqrt{D_{app} C_a (2C_0 - \varepsilon C_a)t} = k\sqrt{t} \quad (1)$$

In Eq. (1), $Q(t)$ represents the cumulative amount of drug released at time t per unit surface area, D_s denotes the drug diffusion coefficient in the release medium, C_0 the total amount of drug in the matrix, C_a the solubility of the drug in the release media, ε the porosity, τ the tortuosity of the matrix, D_{app} the apparent or observed diffusion coefficient ($D_{app} = D_s\varepsilon/\tau$) and k the dissolution rate constant. Drug release can be manipulated by varying: (a) the initial concentration of drug within matrix; (b) porosity; (c) tortuosity; (d) the polymer system forming the matrix; and (e) the solubility of the drug.

Drug release from a porous, hydrophobic polymeric drug delivery system occurs when the drug comes into contact with the release media, subsequently dissolves and diffuses through media filled pores. Thus, the geometry and structure of the pore network are important in this process (Dees and Polderman, 1981; Lowenthal, 1972). The Higuchi model has been reported to fail at drug loading levels below the percolation threshold (Zhang and McGinity, 2000). Below the percolation threshold, incomplete drug release is observed presumably due to limited accessibility of many drug particles to the dissolution medium since they are encapsulated by water insoluble polymeric materials.

The objectives of the present study were to determine the physicochemical properties of ethyl cellulose matrix tablets prepared by either direct compression or hot-melt extrusion in order to explain the drug release mechanism. The influence of compaction force and processing temperature on drug release rates and the physical properties of the tablets was studied. The effect of ethyl cellulose particle size was examined in tablets prepared by both direct compression and hot-melt extrusion. The median pore size, porosity and tortuosity of the matrix tablets prepared by the two techniques were determined using the Webb technique allowing calculation of the diffusion coefficients.

2. Theory of mercury intrusion porosimetry and tortuosity

Knowledge of tortuosity is necessary to determine diffusion coefficients from observed dissolution data. Researchers have relied upon secondary methods to determine tortuosity. These techniques required several steps and were time intensive. Recently, a novel approach using mercury intrusion porosimetry for direct measurement of tortuosity was reported (Webb, 2001b). Mercury intrusion porosimetry has been used to study the pore characteristics of tablets (Gucluyildiz et al., 1977; Selkirk and Ganderton, 1970; Wikberg and Alderborn, 1992), granules (Opakunle and Spring, 1976; Zoglio and Carstensen, 1983), ceramic particles for sustained drug delivery (Byrne and Deasy, 2002) and excipients (Riepma et al., 1993). The technique is based upon the unique properties of mercury. Mercury behaves as a non-wetting liquid toward most substances and will not penetrate a solid unless pressure is applied. For circular pore openings, the Washburn Eq. (2) (Washburn, 1921) relates the applied pres-

sure, P, and the radius, r, of the pores intruded with a non-wetting liquid:

$$r = \frac{-2\gamma \cos\theta}{P} \tag{2}$$

where γ is the surface tension of mercury and θ the contact angle between the liquid and sample. The inverse relationship between pore radius and applied pressure indicates low pressures are used to measure large pore sizes and high pressures are used to measure small pore sizes.

Katz and Thompson (Katz and Thompson, 1986; Thompson et al., 1987) introduced an expression (3) for determination of permeability in porous rocks from mercury intrusion curves based upon concepts from Percolation Theory (Broadbent and Hammersley, 1957; Hammersley, 1957). These researchers found that absolute permeability, K, was related to the rock conductivity at a characteristic length L_c.

$$K = \frac{L_{max}}{89 \times L_c} \phi S(L_{max}) \tag{3}$$

Eq. (3) requires determination of the length at which conductance is at a maximum, L_{max}, and the fraction of total porosity, ϕ, filled at this length $S(L_{max})$. The characteristic length, L_c, is the length at which mercury spans the entire sample and was found to be the point at which percolation begins. It is determined at the point of inflection in the rapidly rising region of the cumulative intrusion curve. Several different scientific disciplines have used the Katz–Thompson method to determine permeability in a variety of materials (Bentz et al., 1998; Berkowitz and Balberg, 1993; Budd, 2002; Celzard et al., 2002; Garboczi and Bentz, 2001).

Jörgen Hager also derived an expression for material permeability based upon a capillary bundle model and knowledge of material tortuosity (Hager, 1998). The capillary bundle model describes the pore network as homogenously distributed in random directions. Using the Hagen–Poiseuille correlation for fluid flow in cylindrical geometries in combination with Darcy's Law, Hager was able to derive an Eq. (4) for permeability, K, in terms of total pore volume, V_{tot}, material density, ρ, pore volume distribution by pore size, $\int_{\eta=r_{c,min}}^{\eta=r_{c,max}} \eta^2 f_v(\eta)\,d\eta$, and material tortuosity, τ. In this method, Hager obtained all parameters except tortuosity from mercury intrusion porosimetry analysis.

$$K = \frac{\rho}{24\tau^2(1+\rho V_{tot})} \int_{\eta=r_{c,min}}^{\eta=r_{c,max}} \eta^2 f_v(\eta)\,d\eta \tag{4}$$

Webb concluded that combining the Hager and Katz–Thompson expressions (Eq. (5)) provided a means for determining tortuosity from mercury intrusion porosimetry data (Webb, 2001a,b).

$$\tau = \sqrt{\frac{\rho}{24K(1+\rho V_{tot})} \int_{\eta=r_{c,min}}^{\eta=r_{c,max}} \eta^2 f_v(\eta)\,d\eta} \tag{5}$$

Since the determination of tortuosity depends upon permeability, changes in material permeability during the analysis will affect the reported value for tortuosity. Webb also reported that improved accuracy was achieved using true density data from helium pycnometry. Thus, the Webb technique allows determination of tortuosity from only two experiments, helium pycnometry and mercury intrusion. The apparent diffusion coefficient and diffusion coefficient can then be calculated using the rate constant from dissolution studies.

3. Experimental

3.1. Materials

Guaifenesin and glacial acetic acid were purchased from Spectrum Laboratory Products (Gardenia, CA). Ethyl cellulose grade Standard 10 (48.0–49.5% ethoxyl substitution, 9–11 cP. viscosity range) was kindly donated by the Dow Chemical Company (Midland, MI). Methanol was purchased from EM Science (Gibbstown, NJ).

3.2. Methods

3.2.1. Preparation of tablets

Ethyl cellulose was sieved into two fractions. The "coarse" fraction included the material that passed through a 30 mesh screen and was retained by an 80 mesh screen. The "fine" fraction included material that passed through 80 mesh screen and was retained on a 325 mesh screen. Guaifenesin was passed through a 30 mesh screen prior to use. The ethyl cellulose particle size fractions were confirmed by introducing an aqueous suspension of ethyl cellulose to laser light scattering using a Malvern Mastersizer S (Malvern Instruments Limited, Malvern, Worcestershire, UK).

A model formulation containing 30% guaifenesin and 70% ethyl cellulose was selected for this study. The drug and polymer were geometrically diluted in a glass mortar and pestle and then introduced into a V Blender (Blend Master®, Patterson-Kelley, East Stroudsburg, PA) and mixed for 15 min. Tablets were prepared from the resultant blend by either direct compression or via hot-melt extrusion.

3.2.2. Direct compression process

Tablet compacts were prepared using a Carver 25 Ton laboratory press (Fred Carver, Menomonee Falls, WI) and a 6 mm diameter flat faced punch and die set. The force applied on the punches was measured using a load cell (ISI Inc., Round Rock, TX) mounted directly on the press with strain gauge sensors. Tablets weighing 250 ± 5 mg were compressed to 10, 30 or 50 kN for 3 s and ejected from the die.

3.2.3. Hot-melt extrusion process

The powder blend was fed into a single-screw Randcastle Extruder (Model RC 0750, Cedar Grove, NJ) equipped with a Nitralloy 135M screw (3:1 compression ratio with flight configuration containing feed, compression and mixing sections) and a rod shaped die (6 mm in diameter). The screw speed was 20 rpm. The three heating zones and die temperatures were set and allowed to equilibrate. Samples were prepared using two different processing temperature ranges: "low" (80, 85, 85, 90 °C) and "high" (90, 105, 105, 110 °C). The residence time of the materials in the extruder was approximately 2–3 min. The extrudates were cooled to 45–55 °C and manually cut into tablets weighing 250 ± 5 mg.

3.2.4. In vitro release properties

Dissolution testing was performed using apparatus II on a Van Kel VK7000 Dissolution Tester (VanKel Industries, Edison, NJ) equipped with an auto sampler (Model VK 8000) according to the guaifenesin tablet monograph in USP 24. Six tablets were placed into the dissolution medium (900 ml of purified water) which was maintained at 37 °C by a circulating bath (Van Kel Model 750D) and agitated at 50 rpm. Samples (5 ml) were removed at specified time points over a 12 h period without media replacement.

Samples were analyzed for guaifenesin content using a Waters (Milford, MA) high performance liquid chromatography (HPLC) system with a photodiode array detector (Model 996) extracting at 276 nm. Samples were pre-filtered through a 0.45 μm membrane (Gelman Laboratory, GHP Acrodisc). An auto sampler (Model 717plus) was used to inject 20 μl samples. The data were collected and integrated using Empower® Version 5.0 software. The column was an Alltech Alltima™ C_{18} 3 μm, 150 mm × 4.6 mm. The mobile phase contained a mixture of water:methanol:glacial acetic acid in volume ratios of 600:400:15. The solvents were vacuum filtered through a 0.45 μm nylon membrane and degassed by sonication. The flow rate was 1.0 ml/min. The retention time of the guaifenesin was 4 min. Linearity was demonstrated from 2 to 200 μg/ml ($R^2 \geq 0.997$) and injection repeatability was 0.35% relative standard deviation for 10 injections.

3.2.5. True density by helium pycnometry

The true density of the powder formulations and tablets was determined in triplicate using helium pycnometry (Micromeritics ® AccuPyc 1330 Pycnometer; Norcross, GA). Twelve tablets were placed in a 12 cm^3 sample cup and purged 20 times at 19.85 psi followed by six analytical runs at 19.85 psi. The equilibration rate was 0.0050 psi/min. An equivalent mass of the powder mixtures was measured in the same manner.

3.2.6. Mercury intrusion porosimetry

The bulk density and tortuosity of the tablets were determined using an AutoPore IV 9500 mercury intrusion porosimeter (Micromeritics, Norcross, GA). Incremental volumes of mercury were plotted against pore diameters according to the Washburn Eq. (2). A surface tension value of 485 D/cm was used for mercury and its contact angle was 130°. Twelve tablets were placed in a 5cc bulb penetrometer and pressure was applied from 1 to 15,000 psia, representing pore diameters of 0.012–360 μm. The pressure at each point was allowed to equilibrate for 10 s. Each run was performed in triplicate. Tablets were analyzed prior to and post-dissolution, with the removal of water from the tablets following dissolution by drying to a constant weight under vacuum for a minimum of 72 h.

3.2.7. Percent effective porosity determination

Percent effective porosity, ε was determined according to the Varner technique (Varner, 1991) us-

ing Eq. (6) in which ρ_t is the true density of the tablet as determined by helium pycnometry and ρ_b the bulk density as determined by mercury intrusion porosimetry. Three runs of 12 tablets were analyzed first by helium pycnometry followed by mercury intrusion porosimetry.

$$\varepsilon = \frac{\rho_t - \rho_b}{\rho_b} \quad (6)$$

3.2.8. Modulated differential scanning calorimetry analysis

Temperature modulated differential scanning calorimetry (M-DSC) was used to characterize the thermal properties of the polymer and drug in physical mixtures and hot-melt extrudates. M-DSC analysis was conducted using a Thermal Advantage Model 2920 from TA Instruments (New Castle, DE) equipped with Universal Analysis 2000 software. Ultrahigh purity nitrogen was used as the purge gas at a flow rate of 150 ml/min. The sample was weighed to 10 ± 5 mg and placed in aluminum pans (Kit 0219-0041, Perkin-Elmer Instruments, Norwalk, CT) and crimped with an aluminum lid. The temperature ramp speed was 2 °C/min from 25 to 150 °C for all studies with a modulation rate of 1.592 °C every minute.

3.2.9. Scanning electron microscopy

Scanning electron microscopy was used to study the surface morphology of the hot-melt extruded tablets. The samples were mounted on an aluminum stage using adhesive carbon tape and placed in a low humidity chamber for 12 h prior to analysis. Samples were coated with gold–palladium for 60 s under an argon atmosphere using a Pelco® Model 3 Sputter Coater (Ted Pella Inc., Tusin, CA) in a high vacuum evaporator equipped with an omni-rotary stage tray. Scanning electron microscopy was performed using a Hitachi S-4500 field emission microscope operating at an accelerating voltage of 15 kV and a 15 μA emission current. Images were captured with Quartz® software.

3.2.10. Statistical analysis

One-way analysis of variance (ANOVA) was used to determine statistically significant differences between results. Results with P-values <0.05 were considered statistically significant ($\alpha = 0.05$). Dissolution curves were analyzed by the model independent approach of Moore and Flanner for dissolution curve comparison using the similarity (f_1) and difference factors (f_2) (Moore and Flanner, 1996).

4. Results and discussion

4.1. The influence of ethyl cellulose particle size on drug release

The influence of ethyl cellulose particle size and processing conditions on the release rate of guaifenesin from matrix tablets was studied. The influence of ethyl cellulose particle size, compaction force and extrusion temperature on guaifenesin release rate is presented in Fig. 1. The guaifenesin release rate from the matrix was highly dependent upon ethyl cellulose particle size and the processing conditions employed to prepare the tablet. In both cases, slower release rates were observed with small particle size ethyl cellulose.

According to Percolation Theory, when a matrix is composed of a water soluble drug and a water insoluble polymer, drug release occurs by dissolution of the active ingredient through capillaries composed of interconnecting drug particle clusters and the pore network (Holman and Leuenberger, 1988; Leuenberger et al., 1987). As drug release continues, the interconnecting clusters increase the pore network through which interior drug clusters can diffuse. The total number of ethyl cellulose particles increases when its particle size is reduced. With more ethyl cellulose particles present, the theory predicts that fewer clusters of soluble drug substance are formed. Furthermore, the presence of finite drug clusters (encapsulated drug particles) is more statistically plausible. The resulting pore network becomes less extensive and more tortuous resulting in slower drug release.

Mercury porosimetry and helium pycnometry were used to determine the pore characteristics and tortuosity of the tablets prior to dissolution testing. The median pore radius, percent effective porosity and tortuosity of the matrix tablets are presented in Table 1. Statistically significant differences in median pore radius ($n = 3$, $P < 0.006$), porosity ($n = 3$, $P < 0.02$) and tortuosity ($n = 3$, $P < 0.009$) were observed between matrix tablets prepared with “fine”

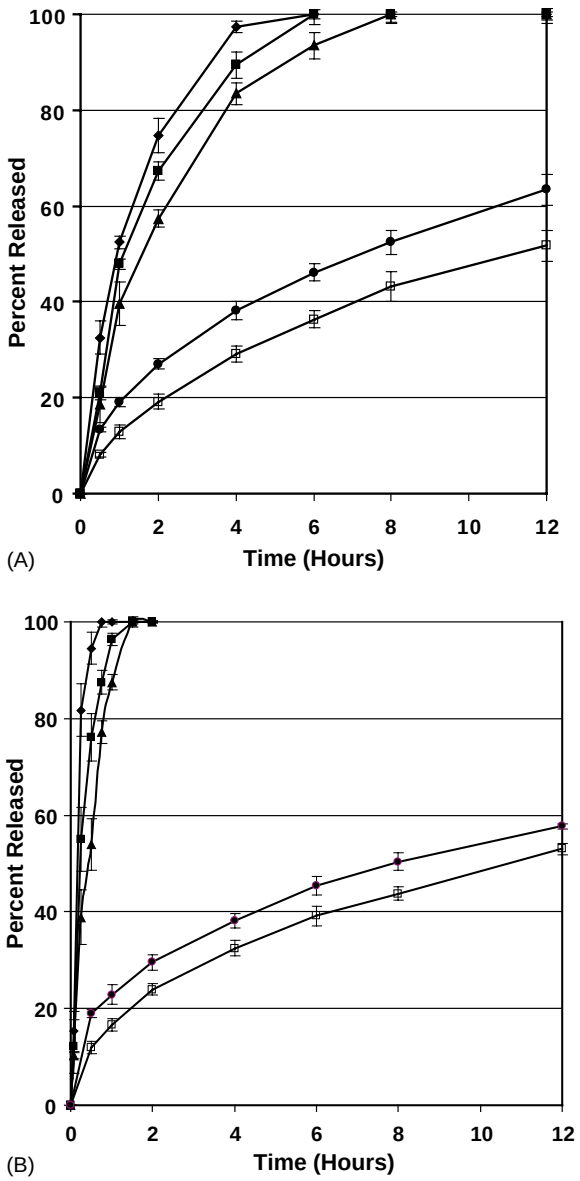

Fig. 1. Influence of ethyl cellulose particle size, compaction force and extrusion temperature on guaifenesin release from matrix tablets prepared by direct compression and hot-melt extrusion containing 30% guaifenesin and 70% ethyl cellulose using USP Method II at 37 °C and 50 rpm in 900 ml of purified water. Each point represents the mean ± standard deviation, $n = 6$. (A) Matrix tablets prepared using "fine" ethyl cellulose (325–80 mesh) and (B) matrix tablets prepared using "coarse" ethyl cellulose (80–30 mesh). (◆) Direct compression, 10 kN; (■) direct compression, 30 kN; (▲) direct compression, 50 kN; (●) hot-melt extrusion, 80, 85, 85, 90 °C; (□) hot-melt extrusion, 90, 105, 105, 110 °C.

and "coarse" ethyl cellulose particle sizes. The median pore radius was smaller, the tablets less porous and more tortuous when prepared with "fine" ethyl cellulose (137–529 Å, 0.4–4.1% porosity and 4.7–321 tortuosity) than in tablets prepared with "coarse" ethyl cellulose (351–1439 Å, 0.7–6.5% porosity and 1.3–125 tortuosity). These data are supported by the dissolution results.

Katikaneni and coworkers (Katikaneni et al., 1995a,b; Upadrashta et al., 1993, 1994) reported that pseudoephedrine hydrochloride release from ethyl cellulose matrix tablets prepared by direct compression was controlled by ethyl cellulose particle size and compression force. These authors concluded that the drug release rate decreased due to a reduction in porosity and increased matrix tortuosity at high compaction forces or when a finer particle of size ethyl cellulose was used. The findings in the present study confirm the work of Katikaneni, support the predictions of Percolation Theory and demonstrate the utility of the mercury porosimetry technique for determination of tortuosity.

Generally, pore radii greater than 200 Å are necessary to avoid hindered diffusion (Anderson and Quinn, 1974). Hindered diffusion can be due to steric exclusion or hindered particle motion. In these situations, either the pore radii are sufficiently small that the molecular dimensions of the solute restrict its diffusion or excessive frictional resistance is created. Hindered diffusion is typically observed when values of the particle radius to pore wall radius ratio are greater than 0.1. The molecular dimensions of guaifenesin were modeled using SAVOL3 software to assess the likelihood of hindered diffusion (Pearlman and Skell, 2003). Assuming a spherical shape, guaifenesin was found to have a radius of 3.53 Å excluding a solvent radius and 5.44 Å with a solvent radius. Assuming an ovoid shape and including a solvent radius, the model predicted the major axis to be 7.84 Å, the first minor axis to be 6.13 Å and the second minor axis to be 3.89 Å. Thus, the minimum guaifenesin particle radius to pore radius ratio is 0.04 in the case of the hot-melt extruded tablets prepared using "fine" ethyl cellulose and processed at 90–110 °C. This value is sufficiently small that hindered diffusion can be considered negligible.

Several assumptions are made using the mercury porosimetry technique which can introduce consid-

Table 1
Median pore radius, percent porosity and tortuosity of matrix tablets prepared by direct compression (DC) and hot-melt extrusion (HME) containing 30% guaifenesin and 70% ethyl cellulose measured before and after dissolution testing

Processing conditions	Median pore radius (Å)		Percent porosity		Tortuosity	
	Before	After	Before	After	Before	After
"Fine" ethyl cellulose (325–80 mesh)						
DC 10 kN	529 ± 24		4.1 ± 0.3		4.7 ± 1.1	
DC 30 kN	476 ± 26		3.8 ± 0.2		6.0 ± 0.6	
DC 50 kN	475 ± 17		3.1 ± 0.2		6.9 ± 0.9	
HME 80, 85, 85, 90 °C	264 ± 8	575 ± 51	1.0 ± 0.2	8.1 ± 1.8	53.2 ± 8.1	4.7 ± 0.6
HME 90, 105, 105, 110 °C	137 ± 6	521 ± 65	0.4 ± 0.2	7.8 ± 2.2	321 ± 22	5.2 ± 0.9
"Coarse" ethyl cellulose (80–30 mesh)						
DC 10 kN	1439 ± 42		6.5 ± 0.2		1.3 ± 0.7	
DC 30 kN	906 ± 23		5.7 ± 0.3		2.1 ± 0.6	
DC 50 kN	710 ± 25		5.2 ± 0.2		2.8 ± 0.5	
HME 80, 85, 85, 90 °C	392 ± 11	642 ± 48	2.3 ± 0.4	8.7 ± 1.4	41.8 ± 5.5	4.4 ± 0.3
HME 90, 105, 105, 110 °C	351 ± 13	588 ± 57	0.7 ± 0.1	8.0 ± 1.1	125 ± 16	5.0 ± 1.1

Each point represents the mean ± standard deviation, $n = 3$.

erable error into the measurements. The assumption of circular pore cross-sections or "cylindrical pore geometry" is due to mathematical convenience in order to avoid complexities calculating mean radii and contact angles in irregularly shaped pores. As a result, the technique is biased to calculate smaller pore sizes than are actually present. Furthermore, "ink bottle pores" also bias the pore size calculation to the small side. Ink bottle pores are defined as pores in which the diameter increases as one moves to its inner dimensions (Leon, 1998; Salmas and Androutsopoulos, 2001). Mercury intrusion also involves subjecting the tablets to equal pressures from 360° as the mercury is forced inside. This means that as mercury intrudes into the pores, the walls of pores penetrated by mercury at a given pressure are uniformly affected by the same pressure. This makes collapse of a pore wall unlikely. However, the tablet can compress under the applied pressure which allows for additional mercury to intrude. This also biases measurement to calculation of smaller than actual pore size. Obviously, the compression of ethyl cellulose is a concern using this technique. To minimize the impact of tablet compression, the applied pressure was not allowed to exceed that applied during the direct compression experiments (50 kN or 15,000 psia). Despite these limitations, pore size information obtained from mercury porosimetry experiments has been consistently demonstrated to be representative.

4.2. The Influence of tableting technique on drug release

Guaifenesin release rates were considerably slower in tablets prepared by hot-melt extrusion than those prepared by direct compression as shown in Fig. 1. Statistically significant differences in median pore radius ($n = 3$, $P < 0.006$), percent effective porosity ($n = 3$, $P < 0.002$) and tortuosity ($n = 3$, $P < 0.0004$) were observed between the direct compression and hot-melt extruded tablets as shown in Table 1. The median pore radius was smaller and the tablets less porous when prepared by hot-melt extrusion (137–392 Å, 0.4–2.3% porosity and 41.8–321 tortuosity) than by direct compression (475–1439 Å, 3.1–6.5% porosity and 1.3–6.9 tortuosity). Adsorption and binding studies did not reveal any interactions. Complete drug recovery was obtained in samples dissolved in ethanol. Thus, the differences in release rate are due to the bonding mechanism of the particles in the two tableting techniques. Ethyl cellulose has been reported to be ductile and the predominant mechanism during compaction is plastic deformation (Katikaneni et al., 1995b). During hot-melt extrusion, solid bridges are formed upon cooling.

The extrusion temperatures were above the melting point of guaifenesin but below the glass transition temperature of ethyl cellulose. The molten drug can act as a solvent for the polymeric particles. Polymeric

particles that do not go into solution are softened at elevated temperatures and deformed by the rotating screw during extrusion. Upon cooling, extensive solid bridges are formed between the particles resulting in a smaller pore radius and more tortuous network. These results demonstrate that densification of the molten mass during extrusion occurs to a greater extent relative to compaction of the powder during compression.

Thermal treatment of amorphous polymers has also been shown to decrease polymer free volume (Follonier et al., 1995). Elevated temperatures and high pressures during hot-melt extrusion followed by cooling significantly impact the free volume. Polymer chain motion and free volume increase with temperature allowing molten guaifenesin molecules to enter these voids. Upon cooling, the guaifenesin molecules remain dispersed in these domains. The net effect is an increase in the degree of packing and a reduction in free volume. Diffusion of molecules through amorphous polymers is governed by free volume and packing. Thus, a decrease in drug transport is anticipated when the free volume decreases and packing order increases.

The miscibility of guaifenesin in ethyl cellulose was studied by modulated differential scanning calorimetry. The glass transition temperature of ethyl cellulose was found to be 129.3 °C (Fig. 2A) and the melting point of guaifenesin was found to be 85.6 °C (Fig. 2B). The melting point of guaifenesin can be observed in the thermograms of the physical mixtures (Fig. 2C and F). Thermograms of the hot-melt extrudates processed at 80–90 °C show a melt transition about 9 °C

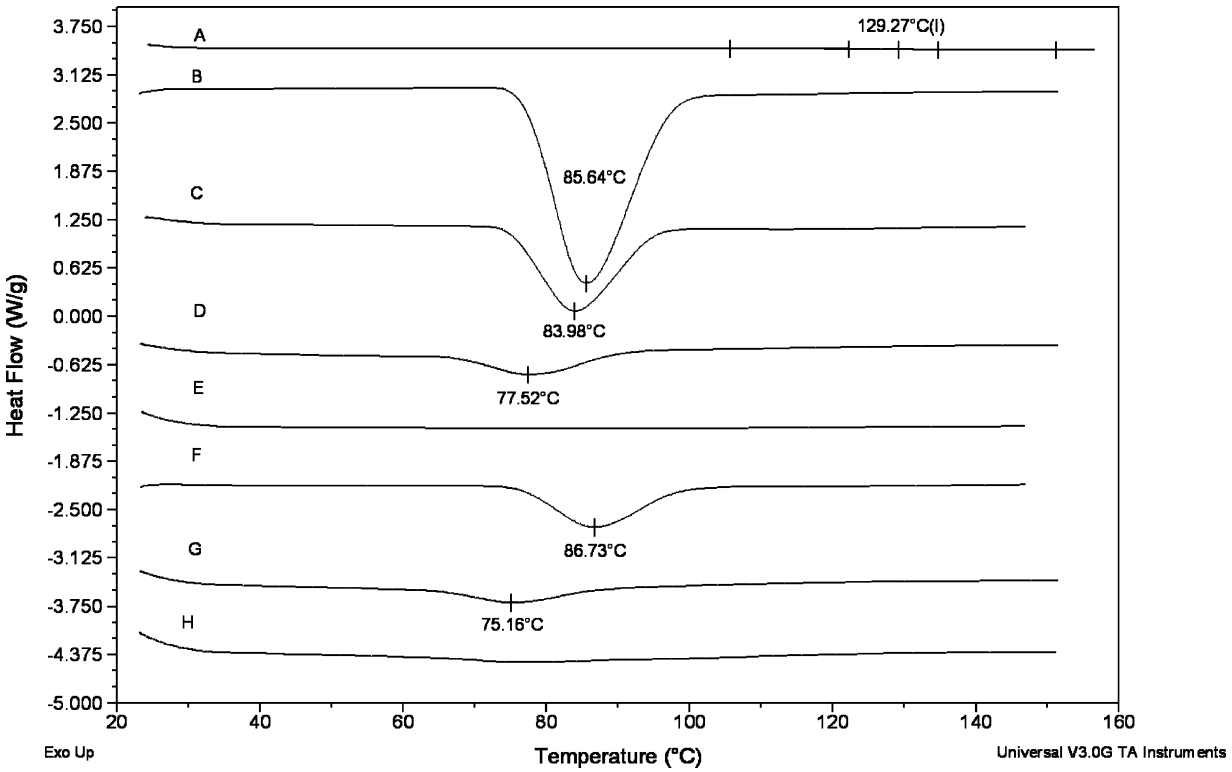

Fig. 2. Modulated differential scanning calorimetry profiles of ethyl cellulose, guaifenesin, physical mixtures and hot-melt extrudates. (A) Ethyl cellulose; (B) guaifenesin; (C) physical mixture of 30% guaifenesin and 70% "coarse" ethyl cellulose; (D) hot-melt extrudate of 30% guaifenesin and 70% "coarse" ethyl cellulose processed at 80, 85, 85, 90 °C; (E) hot-melt extrudate of 30% guaifenesin and 70% "coarse" ethyl cellulose processed at 90, 105, 105, 110 °C; (F) physical mixture of 30% guaifenesin and 70% "fine" ethyl cellulose; (G) hot-melt extrudate of 30% guaifenesin and 70% "fine" ethyl cellulose processed at 80, 85, 85, 90 °C; (H) hot-melt extrudate of 30% guaifenesin and 70% "fine" ethyl cellulose processed at 90, 105, 105, 110 °C.

below the melting point of guaifenesin (Fig. 2D and G). Thermal transitions corresponding to the melting point of guaifenesin are not observed in the extrudates processed at 90–100 °C (Fig. 2E and H). These results indicate that guaifenesin was miscible with ethyl cellulose while in the molten state. The presence of a transition in the hot-melt extrudates processed at 80–90 °C suggests that a two phase solid dispersion was formed in which guaifenesin was present in both amorphous and crystalline form. The absence of a transition in the extrudates processed at higher temperatures suggests the formation of a solid solution.

4.3. The influence of compaction force on drug release

The release rate of guaifenesin decreased with increasing compaction force in tablets prepared by direct compression (Fig. 1). At higher compaction forces, the powder bed densifies to a greater extent and eliminates more of the air in the powder bed and voids in individual particles. The increased densification process results in a tablet with greater mechanical strength, lower porosity and higher tortuosity. These results were confirmed by the helium pycnometry and mercury porosimetry measurements (Table 1). The median pore radius and percent effective porosity decreased and tortuosity increased as the compaction force was raised.

4.4. The influence of hot-melt extrusion temperature on drug release

The guaifenesin release rate in hot-melt extruded tablets decreased as the extrusion temperature increased. Guaifenesin release rates from matrix tablets extruded at 80–90 °C were statistically different from those prepared at 90–110 °C, according to the model independent approach ($f_1 = 29.3$ and $f_2 = 30.6$). Statistically significant differences in median pore radius ($n = 3$, $P < 0.01$), percent effective porosity ($n = 3$, $P < 0.0002$) and tortuosity ($n = 3$, $P < 0.002$) were observed between tablets prepared at the two extrusion temperatures. The median pore radius was larger, the tablets more porous and less tortuous when extruded at 80–90 °C (264–392 Å, 1.0–2.3% porosity and 41.8–53.2 tortuous) than when extruded at 90–110 °C (137–351 Å, 0.4–0.7% porosity and 125–321 tortuous).

Modulated differential scanning calorimetry revealed small melting transitions in the extrudates processed at low temperatures (Fig. 2D and G). These thermal events were absent in the extrudates processed at higher temperatures suggesting that a molecular dispersion was formed to a greater extent at higher extrusion temperatures. Since both processing temperatures were above the melting point of guaifenesin but below the glass transition temperature of ethyl cellulose, it is likely guaifenesin dissolved the ethyl cellulose particles more readily at higher temperatures. The resulting solid dispersion was less porous and more tortuous than that formed at lower processing temperatures.

The stability of polymers used in hot-melt extrusion has been previously investigated (Crowley et al., 2002; Follonier et al., 1994; Repka and McGinity, 2000; Zhang and McGinity, 2000). The stability of ethyl cellulose during hot-melt extrusion by measuring molecular weight using gel permeation chromatography has been described (Brookshaw et al., 1973; De Brabander et al., 2002; Dubernet et al., 1990; Follonier et al., 1995). These researchers report that ethyl cellulose molecular weight was stable during extrusion within the processing conditions employed in this study. Degradation of ethyl cellulose was observed at high temperatures. The onset of degradation of ethyl cellulose was found to occur at ∼190 °C and discoloration at temperatures above 205 °C.

Scanning electron microscopy was used to investigate the surface morphology of the hot-melt extruded matrix tablets prior to dissolution testing and the data are presented in Fig. 3. The surface morphology of the hot-melt extruded tablets was found to depend upon extrusion temperature. At low extrusion temperatures, individual particles are visible (Fig. 3A and C). These particles are likely responsible for the weak melting transitions observed in the DSC experiments (Fig. 2D and G). Few particles and pores are visible and the tablet surface was found to have a striated appearance (Fig. 3B and D) when processed at higher processing temperatures. The striated appearance is the result of “rifling” or shearing of the molten mass on the die wall upon exit from the extruder (Fig. 3E).

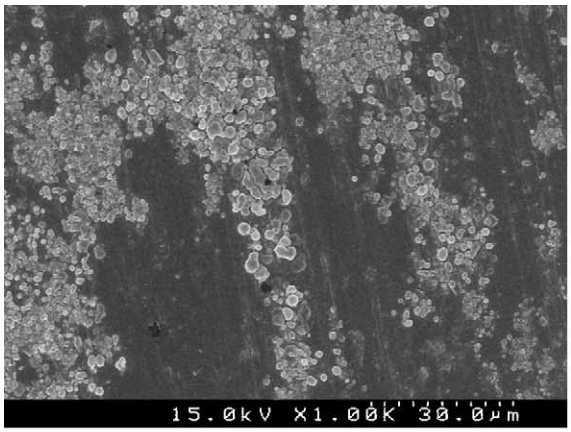

(A)

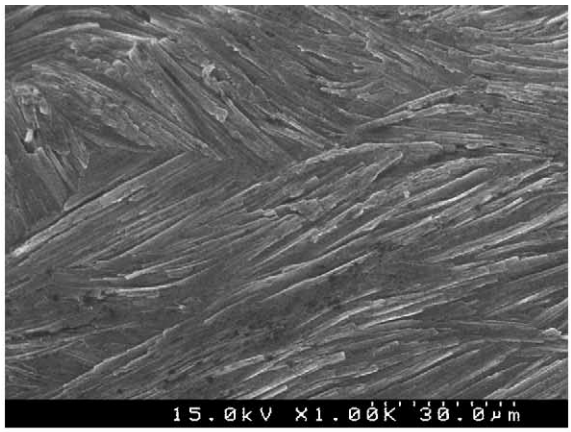

(B)

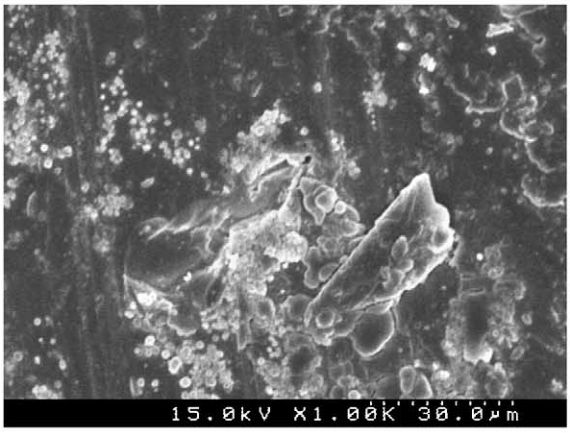

(C)

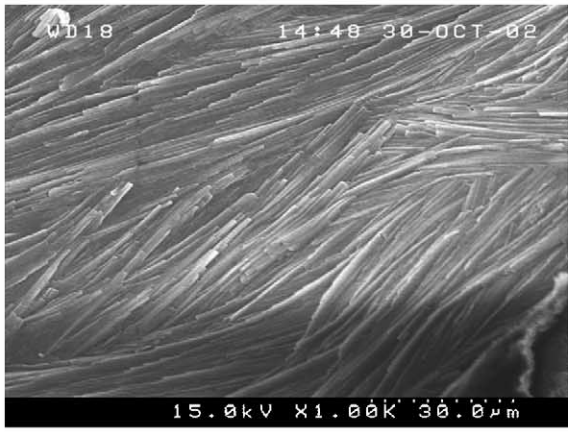

(D)

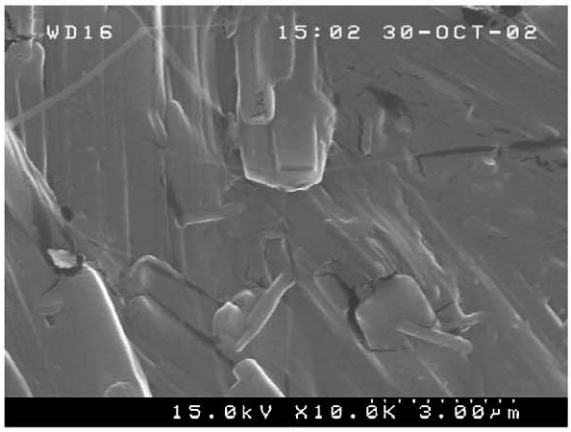

(E)

Fig. 3. SEM micrographs of the surface of hot-melt extruded matrix tablets. (A) Hot-melt extrudate of 30% guaifenesin and 70% “fine” ethyl cellulose processed at 80, 85, 85, 90 °C viewed at 1000× magnification; (B) hot-melt extrudate of 30% guaifenesin and 70% “fine” ethyl cellulose processed at 90, 105, 105, 110 °C viewed at 1000× magnification; (C) hot-melt extrudate of 30% guaifenesin and 70% “coarse” ethyl cellulose processed at 80, 85, 85, 90 °C viewed at 1000× magnification; (D) hot-melt extrudate of 30% guaifenesin and 70% “coarse” ethyl cellulose processed at 90, 105, 105, 110 °C viewed at 1000× magnification; (E) hot-melt extrudate of 30% guaifenesin and 70% “coarse” ethyl cellulose processed at 90, 105, 105, 110 °C viewed at 10,000× magnification.

4.5. Pore characteristics prior to and after dissolution testing

The pore characteristics of the hot-melt extruded matrix tablets measured after dissolution testing are reported in Table 1. Tablets prepared by direct compression could not be analyzed due to matrix erosion and disintegration during dissolution testing. Statistically significant differences were observed in median pore radius ($n = 3$, $P < 0.01$), percent effective porosity ($n = 3$, $P < 0.0006$) and tortuosity ($n = 3$, $P < 0.00004$). Following dissolution testing, the median pore radius increased from 137–392 to 521–642 Å, the porosity increased from 0.4–2.3 to 7.8–8.7%, and the tortuosity decreased from 53.2–321 to 4.4–5.2. Prior to dissolution testing, the pores are primarily voids within the matrix. Following dissolution, the increase in median pore size and porosity is due to capillary diffusion of guaifenesin from the matrix. As guaifenesin particles on the outer surface of the tablet diffuse, a less tortuous pore network is created.

The surface morphology of the hot-melt extruded matrix tablets following a 24 h dissolution test is presented in Fig. 4. When viewed at 1000× magnification, the tablet surface was found to be smooth and no pores were visible. However, when viewed at 10,000× magnification, pores were clearly evident. The tablet surface after dissolution testing was smoother due to hydrodynamic shearing forces from the agitated dissolution medium and the greater number of pores is due to capillary diffusion of guaifenesin.

4.6. Determination of drug release kinetics

The dissolution data were plotted according to the Higuchi equation (Fig. 5) and the kinetic data are shown in Table 2. A higher deviation from the theoretical prediction was observed for matrix tablets prepared by direct compression using “coarse” ethyl cellulose at low compaction forces. The mechanism of release from these tablets was due to both diffusion, erosion and polymer relaxation. These tablets possessed very large pores and were considerably more porous and less tortuous than tablets prepared with “fine” ethyl cellulose. The tablets prepared by direct compression were completely eroded at the conclusion of the dissolution test, irrespective of the particle size of ethyl cellulose.

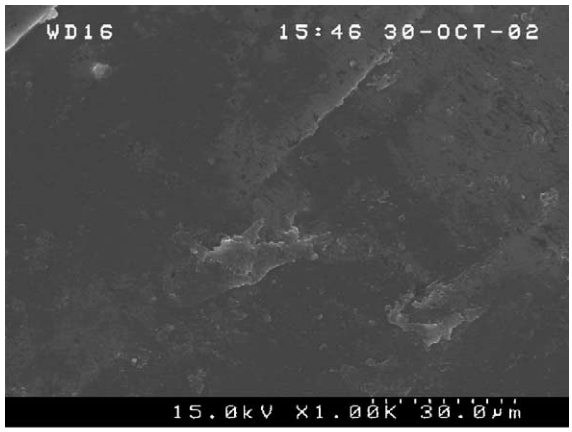

(A)

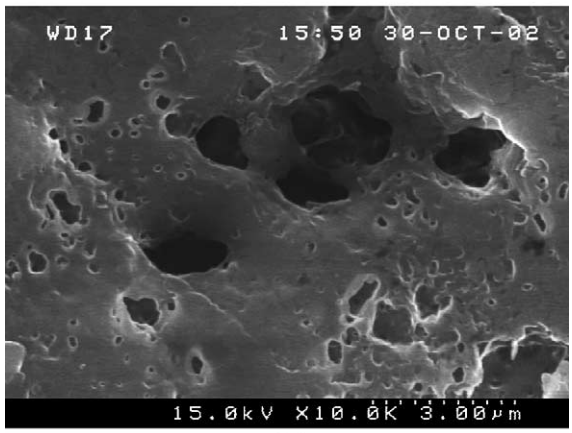

(B)

Fig. 4. SEM micrographs of the surface of hot-melt extruded matrix tablets measured after 24 h dissolution testing. (A) Hot-melt extrudate of 30% guaifenesin and 70% “coarse” ethyl cellulose processed at 90, 105, 105, 110 °C at 1000× magnification following 24 dissolution testing and (B) hot-melt extrudate of 30% guaifenesin and 70% “coarse” ethyl cellulose processed at 90, 105, 105, 110 °C at 10,000× magnification following 24 dissolution testing.

Tablets prepared by direct compression exhibited a burst effect while tablets prepared by hot-melt extrusion demonstrated much slower drug release and a lag time was present. The initial burst effect is indicated by a negative time intercept and a lag is indicated by the positive time intercept on the regression lines determined by the Higuchi model. The burst effect is the result of rapid dissolution and release of drug on the outer surfaces of the tablet. Lag times correspond

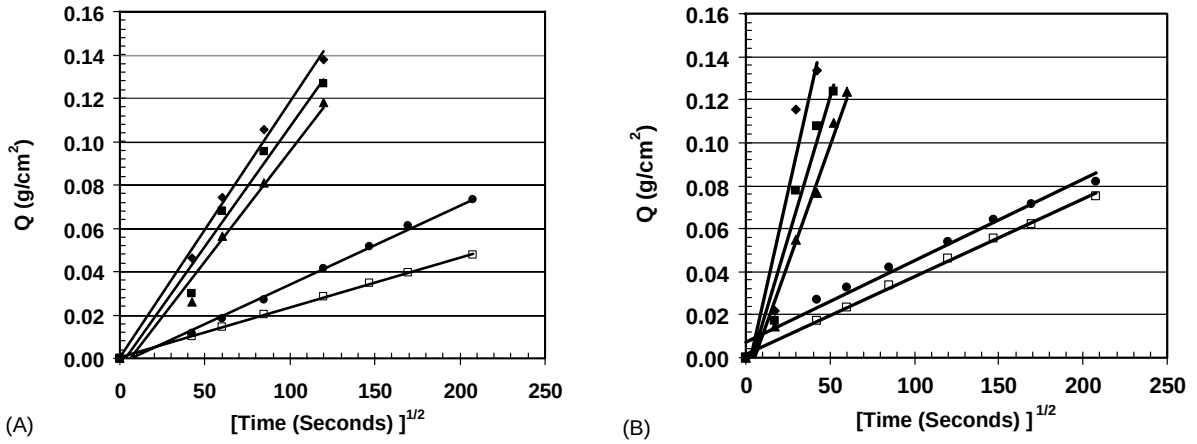

Fig. 5. Higuchi diffusion model fitting of the guaifenesin release data from matrix tablets prepared by direct compression and hot-melt extrusion. (A) Matrix tablets prepared using "fine" ethyl cellulose (325–80 mesh) and (B) matrix tablets prepared using "coarse" ethyl cellulose (80–30 mesh). (◆) Direct compression, 10 kN; (■) direct compression, 30 kN; (▲) direct compression, 50 kN; (●) hot-melt extrusion, 80, 85, 85, 90 °C; (□) hot-melt extrusion, 90, 105, 105, 110 °C.

Table 2
Kinetic data from regression fitting to Higuchi diffusion model giving the rate constant k (g/cm^2 s$^{1/2}$), the y-intercept (g/cm^2), the correlation coefficient r^2, the apparent diffusion coefficient D_{app} (cm^2/s) and the diffusion coefficient D_s from the plot of drug release (g/cm^2) against the square root of time (s$^{1/2}$)

Processing conditions	k (g/cm^2 s$^{1/2}$) $\times 10^3$	y-intercept (g/cm^2) $\times 10^3$	r^2	D_{app} (cm^2/s) $\times 10^6$	D_s (cm^2/s) $\times 10^3$
"Fine" ethyl cellulose (325–80 mesh)					
DC 10 kN	1.18	−0.04	0.995	86.6	9.9
DC 30 kN	1.10	−4.03	0.975	75.2	11.9
DC 50 kN	1.01	−6.02	0.981	63.1	14.1
HME 80, 85, 85, 90 °C	0.43	0.85	0.999	11.3	60.2
HME 90, 105, 105, 110 °C	0.37	0.25	0.997	8.35	669.7
"Coarse" ethyl cellulose (80–30 mesh)					
DC 10 kN	3.08	−4.68	0.899	598	12.0
DC 30 kN	2.48	−6.32	0.961	386	14.2
DC 50 kN	2.19	−10.4	0.971	300	16.2
HME 80, 85, 85, 90 °C	0.38	7.21	0.980	8.90	16.2
HME 90, 105, 105, 110 °C	0.36	1.69	0.998	7.91	141.3

to the time necessary for the dissolution medium to wet the tablet matrix and enter the pores. The hot-melt extruded tablets have a lag time because they have a smaller pore size, are less porous and more tortuous.

5. Conclusions

The results of this study demonstrate that the guaifenesin release rate was dependent upon the particle size of ethyl cellulose and the processing conditions employed to prepare the tablets. The guaifenesin release rate was slower in tablets prepared with the "fine" ethyl cellulose particle size fraction due to the presence of fewer soluble drug clusters within the matrix. Tablets prepared by hot-melt extrusion exhibited considerably slower drug release relative to those prepared by direct compression. Thermal analysis demonstrated that guaifenesin was dispersed in ethyl cellulose at the molecular level in tablets prepared by hot-melt extrusion. The surface morphology of the hot-melt extruded tablets was found to depend upon processing tempera-

ture. The guaifenesin release rate also decreased with increasing compaction force in tablets prepared by direct compression due to greater densification of the powder bed. Analysis of the tablet pore characteristics could be correlated to the observed dissolution results. The Higuchi diffusion model was found to be in good agreement with the drug release profiles for hot-melt extruded tablets. Tablets prepared by direct compression using "coarse" ethyl cellulose were found to release guaifenesin by both diffusion and erosion.

Acknowledgements

The authors would like to thank Glen Baum and the Department of Petroleum Engineering at the University of Texas at Austin for use of their Mercury Porosimeter. The authors wish to express their gratitude and appreciation to Robert S. Pearlman, Ph.D. for his lively discussion and assistance with the SAVOL modeling software. The authors are also grateful to Carrie Crowley, Ingrid Svihla and Lauren Biales for their assistance preparing and testing the tablets. M.M.C. would like to thank the American Foundation for Pharmaceutical Education and the University of Texas at Austin Continuing Fellowship Program for their generous support.

References

AitkenNichol, C., Zhang, F., McGinity, J.W., 1996. Hot melt extrusion of acrylic films. Pharm. Res. 13, 804–808.

Akbuga, J., 1991. Furosemide-loaded ethyl cellulose microspheres prepared by spherical crystallization technique: morphology and release characteristics. Int. J. Pharm. 76, 193–198.

Anderson, J.L., Quinn, J.A., 1974. Restricted transport in small pores. Biophys. J. 14, 130.

Bentz, D.P., Garboczi, E.J., Quenard, D.A., 1998. Modelling drying shrinkage in reconstructed porous materials: application to porous Vycor glass. Model. Simul. Mater. Sci. Eng. 6, 211–236.

Berkowitz, B., Balberg, I., 1993. Percolation Theory and its application to groundwater hydrology. Water Resour. Res. 29, 775–794.

Broadbent, S.R., Hammersley, J.M., 1957. Percolation processes. Part I. Crystals and mazes. Proc. Cambridge Phil. Soc. 53, 629–641.

Brookshaw, A.P., Hillman, D.E., Paul, J.I., 1973. Gel permeation chromatographic evaluation of ethyl cellulose extrudates exhibiting "Sharkskin Effect". Br. Polym. J. 5, 229–239.

Budd, D.A., 2002. The relative roles of compaction and early cementation in the destruction of permeability in carbonate grainstones: a case study from the Paleogene of west-central Florida, USA. J. Sediment. Res. 72, 116–128.

Byrne, R.S., Deasy, P.B., 2002. Use of commercial porous ceramic particles for sustained drug delivery. Int. J. Pharm. 246, 61–73.

Celzard, A., Collas, F., Mareche, J.F., Furdin, G., Rey, I., 2002. Porous electrodes-based double-layer supercapacitors: pore structure versus series resistance. J. Power Sources 108, 153–162.

Crowley, M.M., Zhang, F., Koleng, J.J., McGinity, J.W., 2002. Stability of polyethylene oxide in matrix tablets prepared by hot-melt extrusion. Biomaterials 23, 4241–4248.

De Brabander, C., Van den Mooter, G., Vervaet, C., Remon, J.P., 2002. Characterization of ibuprofen as a nontraditional plasticizer of ethyl cellulose. J. Pharm. Sci. 91, 1678–1685.

Dees, P.J., Polderman, J., 1981. Mercury porosimetry in pharmaceutical technology. Powder Technol. 29, 187–197.

Dubernet, C., Rouland, J.C., Benoit, J.P., 1990. Comparative study of two ethylcellulose forms (raw material and microspheres) carried out through thermal analysis. Int. J. Pharm. 64, 99–107.

Eldridge, J.H., Hammond, C.J., Meulbroek, J.A., Staas, J.K., Gilley, R.M., Tice, T.R., 1990. Controlled vaccine release in the gut-associated lymphoid tissues. Part I. Orally administered biodegradable microspheres target the peyer's patches. J. Control Release 11, 205–214.

Follonier, N., Doelker, E., Cole, E.T., 1994. Evaluation of hot-melt extrusion as a new technique for the production of polymer-based pellets for sustained-release capsules containing high loadings of freely soluble drugs. Drug Dev. Ind. Pharm. 20, 1323–1339.

Follonier, N., Doelker, E., Cole, E.T., 1995. Various ways of modulating the release of diltiazem hydrochloride from hot-melt extruded sustained-release pellets prepared using polymeric materials. J. Control Release 36, 243–250.

Garboczi, E.J., Bentz, D.P., 2001. The effect of statistical fluctuation, finite size error, and digital resolution on the phase percolation and transport properties of the NIST cement hydration model. Cem. Concr. Res. 31, 1501–1514.

Gucluyildiz, H., Banker, G.S., Peck, G.E., 1977. Determination of porosity and pore-size distribution of aspirin tablets relevant to drug stability. J. Pharm. Sci. 66, 407–414.

Hager, J., 1998. Steam Drying of Porous Media. Ph.D. Thesis. Lund University.

Hammersley, J.M., 1957. Percolation processes. Part II. The connective constant. Proc. Cambridge Phil. Soc. 53, 642–645.

Higuchi, T., 1963. Mechanisms of sustained action medication. Theoretical analysis of rate of release of solid drugs dispersed in solid matrices. J. Pharm. Sci. 52, 1145–1149.

Holman, L.E., Leuenberger, H., 1988. The relationship between solid fraction and mechanical properties of compacts—the Percolation Theory Model Approach. Int. J. Pharm. 46, 35–44.

Jalsenjak, I., Nicolaidou, C.F., Nixon, J.R., 1977. Dissolution from tablets prepared using ethyl cellulose microcapsules. J. Pharm. Pharmacol. 29, 169–172.

Katikaneni, P.R., Upadrashta, S.M., Neau, S.H., Mitra, A.K., 1995a. Ethylcellulose matrix controlled release tablets of a water soluble drug. Int. J. Pharm. 123, 119–125.

Katikaneni, P.R., Upadrashta, S.M., Rowlings, C.E., Neau, S.H., Hileman, G.A., 1995b. Consolidation of ethylcellulose: effect of particle size, press speed, and lubricants. Int. J. Pharm. 117, 13–21.

Katz, A.J., Thompson, A.H., 1986. Quantitative prediction of permeability in porous rock. Phys. Rev. B 34, 8179–8181.

Leon, C., 1998. New perspectives in mercury porosimetry. Adv. Colloid Interface Sci. 77, 341–372.

Leuenberger, H., Rohera, B.D., Haas, C., 1987. Percolation Theory—a novel approach to solid dosage form design. Int. J. Pharm. 38, 109–115.

Lowenthal, W., 1972. Disintegration of tablets. J. Pharm. Sci. 61, 1695–1711.

McGinity, J.W., Koleng, J.J., Repka, M.A., Zhang, F., 2000. In: Swarbrick, J., Boilan, J.C. (Eds.), Encyclopedia of Pharmaceutical Technology, vol. 19. Marcel Dekker, New York, pp. 203–226.

Moore, J.W., Flanner, H.H., 1996. Mathematical comparison of dissolution profiles. Pharm. Tech. 20, 64–74.

Opakunle, W.O., Spring, M.S., 1976. Granulation of binary-mixtures—effects of composition of granulating solution and initial particle-size of one-component on granule properties. J. Pharm. Pharmacol. 28, 806–809.

Pearlman, R.S., Skell, J.M., 2003. Savol: molecular surface-areas, volumes, and various atomic-based partitions thereof. Optive Research Inc., http://www.optive.com.

Repka, M.A., McGinity, J.W., 2000. Influence of Vitamin E TPGS on the properties of hydrophilic films produced by hot-melt extrusion. Int. J. Pharm. 202, 63–70.

Riepma, K.A., Vromans, H., Zuurman, K., Lerk, C.F., 1993. The effect of dry granulation on the consolidation and compaction of crystalline lactose. Int. J. Pharm. 97, 29–38.

Rowe, R.C., 1992. Molecular weight dependence of the properties of ethyl cellulose and hydroxypropyl methylcellulose films. Int. J. Pharm. 88, 405–408.

Rubio, M.R., Ghaly, E.S., 1994. In-vitro release of acetaminophen from sodium alginate controlled-release pellets. Drug Dev. Ind. Pharm. 20, 1239–1251.

Salmas, C.E., Androutsopoulos, G.P., 2001. A novel pore structure tortuosity concept based on nitrogen sorption hysteresis data. Ind. Eng. Chem. Res. 40, 721–730.

Selkirk, A.B., Ganderton, D., 1970. The influence of wet and dry granulation methods on the pore structure of lactose tablets. J. Pharm. Pharmacol. 22, 86S–94S.

Shaikh, N.A., Abidi, S.E., Block, L.H., 1987a. Evaluation of ethylcellulose as a matrix for prolonged release formulations. Part 1. Water-soluble drugs—acetaminophen and theophylline. Drug Dev. Ind. Pharm. 13, 1345–1369.

Shaikh, N.A., Abidi, S.E., Block, L.H., 1987b. Evaluation of ethylcellulose as a matrix for prolonged release formulations. Part 2. Sparingly water-soluble drugs—ibuprofen and indomethacin. Drug Dev. Ind. Pharm. 13, 2495–2518.

Thompson, A.H., Katz, A.J., Raschke, R.A., 1987. Mercury injection in porous-media—a resistance devils staircase with percolation geometry. Phys. Rev. Lett. 58, 29–32.

Upadrashta, S.M., Katikaneni, P.R., Hileman, G.A., Keshary, P.R., 1993. Direct compression controlled release tablets using ethylcellulose matrices. Drug Dev. Ind. Pharm. 19, 449–460.

Upadrashta, S.M., Katikaneni, P.R., Hileman, G.A., Neau, S.H., Rowlings, C.E., 1994. Compressibility and compactibility properties of ethylcellulose. Int. J. Pharm. 112, 173–179.

Varner, J., 1991. Descriptive Fractography, Ceramics and Glasses, ASM, Ohio.

Washburn, E.W., 1921. Note on a method of determining the distribution of pore sizes in a porous material. Proc. Natl. Acad. Sci. U.S.A. 7, 115–116.

Webb, P.A., 2001a. AutoPore IV 9500 Operator's Manual V1.04, Micromeritics Instrument Corp.

Webb, P.A., 2001b. An Introduction to the Physical Characterization of Materials by Mercury Intrusion Porosimetry with Emphasis on Reduction and Presentation of Experimental Data. World Wide Web http://www.micromeritics.com/pdf/mercury_paper.pdf (January 2001).

Wikberg, M., Alderborn, G., 1992. Compression characteristics of granulated materials. Part 6. Pore-size distributions, assessed by mercury penetration, of compacts of 2 lactose granulations with different fragmentation propensities. Int. J. Pharm. 84, 191–195.

Young, C.R., Koleng, J.J., McGinity, J.W., 2002. Production of spherical pellets by a hot-melt extrusion and spheronization process. Int. J. Pharm. 242, 87–92.

Zhang, F., McGinity, J.W., 1999. Properties of sustained-release tablets prepared by hot-melt extrusion. Pharm. Dev. Technol. 4, 241–250.

Zhang, F., McGinity, J.W., 2000. Properties of hot-melt extruded theophylline tablets containing poly(vinyl acetate). Drug Dev. Ind. Pharm. 26, 931–942.

Zhang, Y.E., Tchao, R., Schwartz, J.B., 2001. Effect of processing methods and heat treatment on the formation of wax matrix tablets for sustained drug release. Pharm. Dev. Technol. 6, 131–144.

Zoglio, M.A., Carstensen, J.T., 1983. Physical aspects of wet granulation. Part 3. Effect of wet granulation on granule porosity. Drug Dev. Ind. Pharm. 9, 1417–1434.